Journal of Sound and Vibration (1994) **171**(2), 185–200

SLIDING-MODE/SHAPED-INPUT CONTROL OF FLEXIBLE/RIGID LINK ROBOTS

T. SINGH

Mechanical and Aerospace Engineering, SUNY at Buffalo, Buffalo, New York 14260, *U.S.A.*

AND

M. F. GOLNARAGHI AND R. N. DUBEY

Mechanical Engineering, University of Waterloo, Waterloo, Ontario N2L3G1, Canada

(*Received* 22 *January* 1992, *and in final form* 16 *September* 1992)

A controller for a flexible/rigid link robot is designed using the sliding-mode and shaped-input concepts. The controller for the rigid body motion is designed to serve two purposes: it forces the state trajectory onto a preselected sliding surface and then guides it to the state space origin. The shaped-input controller is designed for the control of the flexible motion which requires information about the natural frequency and damping of the linearized system. This information is used to discretize the input so that minimum energy is injected via the controller to the flexible modes of the structure. The controller is tested successfully on an experimental flexible link robot.

1. INTRODUCTION

Distributed parameter systems theory has gained considerable maturity in the past two decades. The origin of this field can be traced back to papers by the Russian scientists Butkovskii and Lerner [1] in 1960. Application areas include chemical engineering, mechanical and civil engineering (bridges, flexible arm robots and large antennas) and even physiology (mathematical modelling of the distribution and effects of drugs in humans). Distributed parameter systems are modelled by partial differential equations. In the case of flexible link robots, the partial differential equations reflect the distributed nature of mass and stiffness. The first impulse of researchers is to simplify the model to a form that is amenable to solution using conventional techniques. Eigenfunction expansion, space quantization, space and time quantization and transfer function approximations are a few of the techniques used to transform the partial differential equations into a set of ordinary differential or difference equations.

Models of realistic systems are seldom completely known and, if known, are rarely linear. Control theorists are now required to design controllers applicable to non-linear, incompletely modelled systems, to systems the models for which can be improved on-line during system operation. The normal procedure for designing controllers for non-linear systems has been to linearize the system and then design a controller for the resulting system. This procedure can yield unsatisfactory performance, especially when the system is highly non-linear and undergoes large motion, as is the case for control of robotic manipulators, advanced aircraft control etc.

0022–460X/94/120185 + 16 $08.00/0

Control of multi-link, flexible arm robots belongs to the class of problems that is characterized by non-linearity and incompleteness in modelling. The incompleteness in modelling is due to the transformation to convert the partial differential equations into a system of ordinary differential equations. The effects of Coriolis, centripetal and gyroscopic terms contribute to the non-linearity in the model. A generalized control strategy is consequently desired to track any command input with minimal vibration of the links. Many investigators have studied various control methods to find a successful and practical control technique for flexible arm robots. The importance of this area is highlighted by the publication of numerous research papers, which is also indicative of the non-availability of a satisfactory control method. There is a plethora of papers on the control of single flexible link robots. Wilson *et al.* [14] designed controllers using the pole placement technique. Vidyasagar and Wang [13] designed a controller using the stable factorization approach. Meirovitch *et al.* [3] designed an on–off controller to control a free–free beam in a non-linear fashion. The use of acceleration feedback was promulgated by Kotnik *et al.* [2]. Gebler *et al.* [7] worked on the control of a two-link flexible arm robot. An optimized reference trajectory for the rigid body is realized using a non-linear feedforward concept: any deviations from this path are counterbalanced by an additional feedforward loop and the remaining elastic vibrations are actively damped by feeding back strain gauge measurements. Oakley and Cannon [5] used a collocated PID control scheme to regulate the motion of a two-link flexible arm robot. The controller was designed to compensate for the effect of Coulomb friction. Oakley and Cannon also designed a collocated PD controller for a two-link manipulator with a very flexible forearm [4]. A self-tuning scheme approach was adopted to resolve the robustness of the system to changes in the system parameters.

The equations of motion of a multi-link robot are non-linear and are not known exactly. Thus, controlling the robot in a decentralized fashion is feasible only if the controller for each joint is robust, first because the model of the system is not exactly known, and, second, because the coupling of the other links in consideration is considered as disturbance. Thus, the controller should be able to reject the disturbance and be robust to handle the discrepancies in the model. Sliding-mode controllers are suitable for the control of systems with uncertainities. A sliding-mode controller has been designed based on a Lyapunov function, to arrive at a control law [9]. The sliding-mode technique may be used in a decentralized fashion, provided that the bounds on the coupling of the other links are known. The sliding-mode technique can also be used to control the non-linear system in a centralized manner. The control technique in this paper uses the latter approach to control the rigid body motion.

Smith [11] proposed discretizing a step input to an underdamped second order system into two steps to cancel any harmonic motion of the system. The basis of this control strategy is to utilize the second step of the discretized step input to annul the vibratory motion of the plant. This is achieved by forcing the response of the second step to be 180 degrees out of phase with the response to the first step. Thus the final position of the system is the position at the time at which the second step is applied. Singer and Seering [8] ameliorated this control strategy by introducing robustness into the controller to variations in estimated damping and frequency. This was achieved by increasing the number of discrete steps, from the two proposed by Smith to three or more: the greater the number of steps, the greater the robustness. The cost of increasing the number of steps is reflected by the increased time to reach the final position. The non-linear nature of the multi-flexible-link system changes the natural frequency of the links with change in position. Thus, the shaped-input controller provides us with a patent choice to attenuate the vibratory motion of the flexible links in a robust fashion.

2. CONTROL PHILOSOPHY

The motion of the multi-link, flexible arm robot is assumed to consist of two parts, the gross or average motion (rigid body motion) and the perturbations about this average motion (vibration of the flexible links). The average motion of the system is controlled using a feedback controller. The perturbations about the mean trajectory will tend to zero as the flexible modes are damped, although lightly. The next step is to accelerate the damping out of the vibrations in an open loop fashion. The sliding-mode and shaped-input controllers are used to exemplify the control philosophy. The sliding-mode caters to the rigid body motion (gross motion) and the shaped-input controller modifies the command input so as to annul any vibrations in the flexible links.

3. CONTROLLER DESIGN

3.1. SLIDING-MODE CONTROLLER

The equations of motion of any robot are linear with respect to the control, that is, the system can be represented in the form

$$\dot{x} = f(x) + B(x)u, \tag{1}$$

where x and f are $2n$-dimensional column vectors, $B(x)$ is a $2n \times m$ matrix, and u is an m-dimensional input vector. It is assumed that the functions $f(n)$ and $B(x)$ satisfy the Lipschitz condition outside the sliding surface. In such systems, sliding motion occurs which, unlike the scalar case, stays on the intersection of the sliding surface rather than on a single sliding surface [12].

The motion of a system controlled by a sliding-mode controller can be described in two phases. The first involves forcing the state trajectory, from any initial condition to a predefined surface; and the second involves sliding along this surface to the state space origin. The design of the controller is also two-fold; selection of a surface to produce the desired dynamics and the selection of a control law that forces the selected surface to be globally attractive.

The equation of motion of a multi-rigid-link robot can be represented as

$$\begin{bmatrix} \dot{x}_1 \\ \dot{x}_2 \end{bmatrix} = \begin{bmatrix} x_2 \\ [M]^{-1}(-[C(x_1, x_2)] - [K]x_1) \end{bmatrix} + \begin{bmatrix} 0 \\ [M]^{-1} \end{bmatrix} u, \tag{2}$$

where M is the mass or inertia matrix, C is the coupling matrix, reflecting the effect of the Coriolis, centripetal and gyroscopic non-linearities, and K is the stiffness matrix. The variables x_1 and x_2 are state vectors of the same dimension. This model is used to design the sliding-mode controller, as this controller caters to the rigid body motion.

The first step is to select the sliding surface. The linear sliding surface selected is of the form

$$\sigma = Sx = 0, \tag{3}$$

where the terms of S are the direction cosines of the normal to the surface(s). The sliding surface is of dimension $(2n - m)$, where $2n$ is the number of states in the system and m is the number of inputs to the system. The final surface can also be considered to be the intersection of m, $(2n - 1)$-dimensional surfaces. The sliding surface can also be represented as

$$\sigma = [S_1 \quad S_2] \begin{Bmatrix} x_1 \\ x_2 \end{Bmatrix} = 0. \tag{4}$$

Since the non-linearities lie in the range space of the input, they can be eliminated when the system state is on the sliding manifold, where the equation of the sliding manifold provides us with an algebraic relation between the states. When the system trajectory is on the surface, that states are related as

$$x_2 = -S_2^{-1} S_1 x_1, \tag{5}$$

assuming that S_2 is non-singular. Substituting equation (5) into the first half of equation (2), we have

$$\dot{x}_1 = -S_2^{-1} S_1 x_1. \tag{6}$$

This is now in a form that can be exploited to select the coefficients of the sliding surface. $S_2^{-1} S_1$ is in the form of the state feedback matrix, and a plethora of techniques is available to select the feedback matrix. Thus the desired dynamics define the sliding surface. When the system state is on the selected suface, the dynamics of the system are defined by the following equations:

$$\dot{x}_1 = -S_2^{-1} S_1 x_1 \qquad \text{and} \qquad x_2 = -S_2^{-1} S_1 x_1. \tag{7, 8}$$

Having selected the surface, the next step is to choose a control law that forces the system state onto this surface. The definition of a sliding-mode resembles the definition of Lyapunov stability, which provides us with a patent choice to select the control law. Let us choose a Lyapunov function $V(x, \sigma)$ of the form

$$V = \tfrac{1}{2} \sigma^{\mathrm{T}} \sigma, \tag{9}$$

which is globally positive definite with respect to the surface σ. To ensure that the surface is globally attractive, the derivative of the Lyapunov function with respect to time should be negative definite; that is,

$$\mathrm{d}V/\mathrm{d}t = \sigma^{\mathrm{T}} \dot{\sigma} < 0, \qquad \mathrm{d}V/\mathrm{d}t = \sigma^{\mathrm{T}} S \dot{x} < 0. \tag{10, 11}$$

On substituting equation (1) into equation (11), we have

$$\mathrm{d}V/\mathrm{d}t = \sigma^{\mathrm{T}} S (f(x) + B(x)u) < 0. \tag{12}$$

We need to select u such that equation (12) is globally negative definite. Let

$$u = -(SB)^{-1} S f(x) - (SB)^{-1} \epsilon \sigma, \tag{13}$$

where ϵ is a diagonal matrix of positive constants, the components of which define how fast the surface is approached. Substitute equation (13) into equation (12) to obtain

$$\mathrm{d}V/\mathrm{d}t = \sigma^{\mathrm{T}} S (f(x) + B(x)(-(SB)^{-1} S f(x) - (SB)^{-1} \epsilon \sigma) < 0. \tag{14}$$

It is simplified to

$$\mathrm{d}V/\mathrm{d}t = -\sum_{i=1}^{m} \sigma_i \sigma_i \epsilon_i, \tag{15}$$

which is negative definite, thus forcing the selected surface to be globally attractive.

3.2. SHAPED INPUT CONTROL

The next step in the design process involves modifying the command input to the system such that the response of the system does not contain any harmonic content. Smith [11], in 1958, proposed breaking up a step input to an underdamped system into two steps, such that the response of the underdamped system was non-oscillatory. Singer and Seering [8] ameliorated this control concept to incoporate robustness to variations in damping and

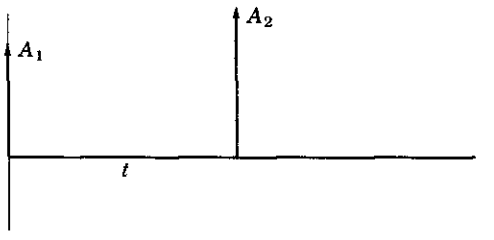

(a)

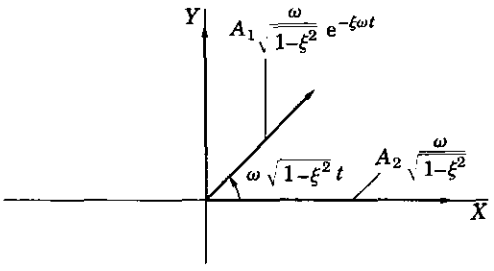

(b)

Figure 1. (a) Impulse sequence; (b) vector diagram illustrating the response of the system to two impulse inputs.

frequency. The vector diagram (Figure 1) is used to exemplify this control concept, which represents the impulse response of a second order system by means of a rotating vector, the projection of which on the y-axis is the impulse response of the system. The vector diagram represents the response of an underdamped system to two impulses. The controller requires determination of the relative amplitudes of the impulses and the time at which they have to be applied, such that the system does not respond in an oscillatory manner. We assume that the second impulse is applied t seconds after the first, which has an amplitude of unity. For the resultant response to be zero, the following two equations must be satisfied simultaneously:

$$(\omega/\sqrt{1-\xi^2})\, e^{-\xi\omega t} \cos(\omega\sqrt{1-\xi^2}\, t) + A_2\omega/\sqrt{1-\xi^2} = 0, \tag{16}$$

and

$$(\omega/\sqrt{1-\xi^2})\, e^{-\xi\omega t} \sin(\omega\sqrt{1-\xi^2}\, t) = 0. \tag{17}$$

We have, from equations (16) and (17),

$$A_2 = \exp\left(\frac{-\xi\pi}{\omega\sqrt{1-\xi^2}}\right), \tag{18}$$

applied at

$$t = \pi/(\omega\sqrt{1-\xi^2}). \tag{19}$$

To produce an aperiodic response to any command input, the impulse sequence is convolved with the command input, and this modified input produces the desired response. This controller can be used to control the motion of a flexible arm robot subject to point-to-point motion. The two-impulse shaped input cancels vibrations only if the natural frequency and damping of the system are exactly known. Singhose *et al.* [10] proposed to minimize the sum of the components of the system response vectors in the X and Y

TABLE 1

Impulse sequence

Time (s)	Amplitude of step
0·0	1
$\frac{\pi}{\omega\sqrt{1-\xi^2}}$	$2e^{-\xi\pi/\sqrt{1-\xi^2}}$
$2\frac{\pi}{\omega\sqrt{1-\xi^2}}$	$(e^{-\xi\pi/\sqrt{1-\xi^2}})^2$

(Figure 1) directions to variations in frequency. To achieve their objective, they proposed a three-impulse controller, whose relative amplitudes, for zero initial conditions are derived in the same fashion as the two-impulse sequence and are listed in Table 1.

The natural frequencies of multi-flexible-link robots are functions of the link positions, implying that the natural frequencies change with the link position. Since the shaped-input controller is robust with respect to variations in natural frequencies, it can be used to eliminate the oscillatory portion of the response. This control strategy is tested on an experimental single flexible-link robot, the results of which are presented next.

4. EXPERIMENTAL RESULTS

The testbed for the proposed control strategy, is a two-flexible-link mechanism. Each link is driven by a d.c. servo motor. The first link (72·6 × 10·16 × 0·3172 cm) is less flexible

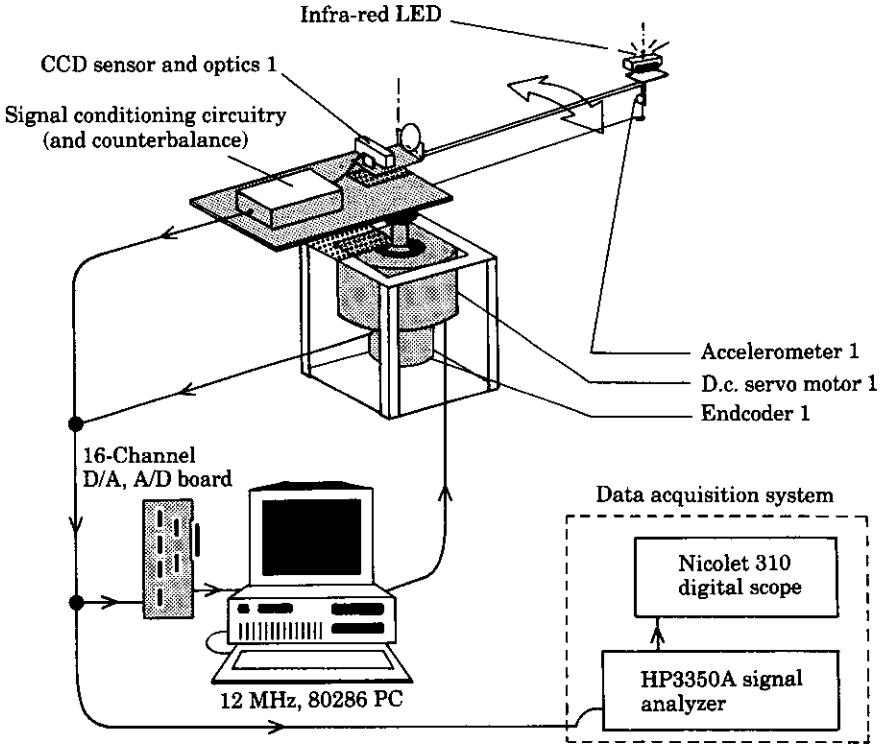

Figure 2. Schematic of flexible link manipulator configuration.

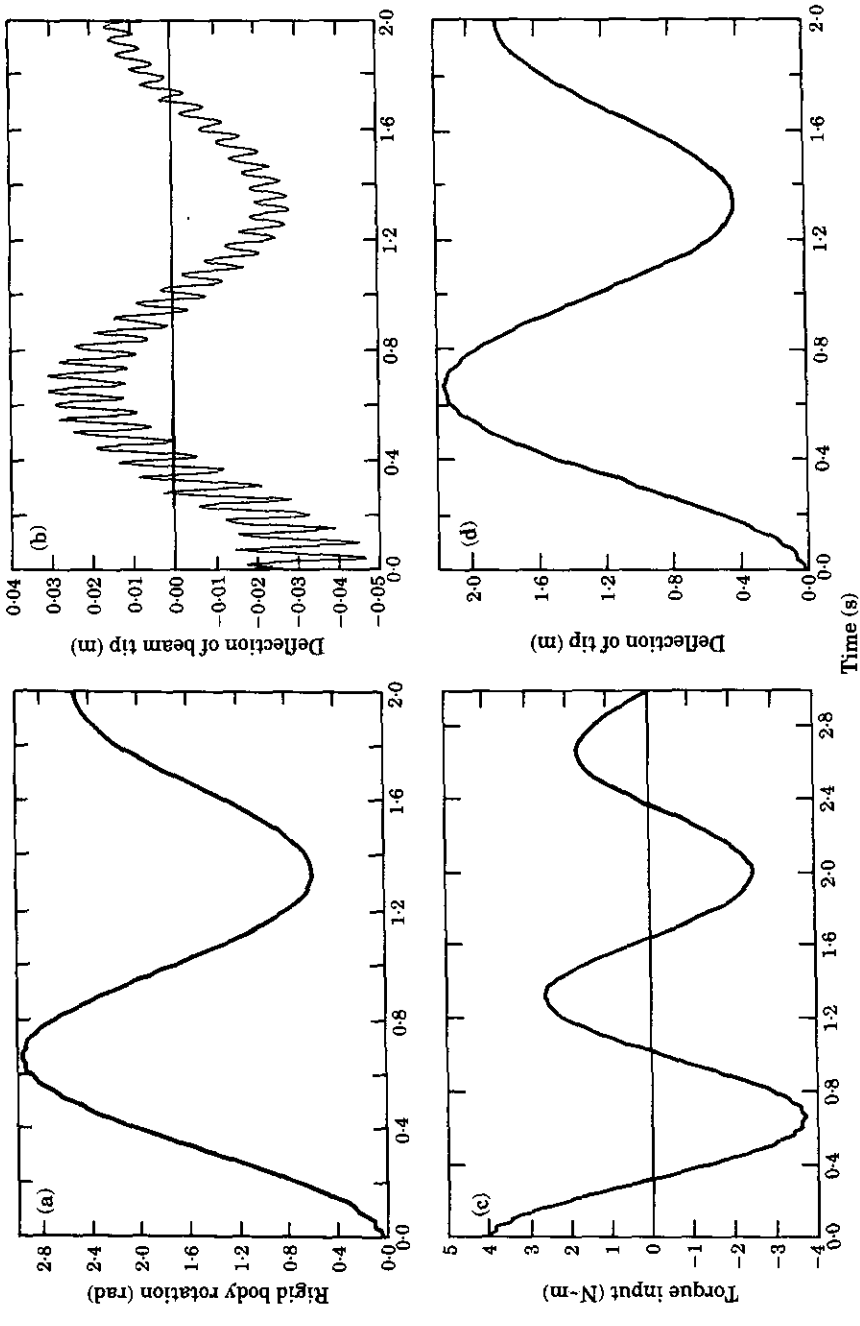

Figure 3. Experimental results for a PD controller: (a) rigid body response; (b) tip deflection of link; (c) control input history; (d) arc traversed by tip of link.

TABLE 2

Three-impulse sequence convolved with a step input

Time (s)	Amplitude of step (rad)
0·0	0·4113
0·6545	1·1961
1·3089	1·5707

compared to the second link ($50 \times 2{\cdot}54 \times 0{\cdot}1587$ cm) and is driven directly by a servo motor (Inertial Motors Model GA4552-1), unlike the second link which employs a gear train to enable the use of a smaller motor (Electro-Craft, Inc. Model E350-MGH) (Figure 2). The sensory system comprises two cameras to detect the deflection of the tip of the links from their rigid body positions. The CCD cameras, which are integral with the shaft of the motors, detect the deflection via infra-red light emitting diodes mounted at the tip of the links. Optical encoders (SUNX REX-31), used in conjunction with a HCTL-2000 quadrature decoder counter, and tachometers are used to measure the position and velocity of the motor shaft, respectively. The mechanical hardware is interfaced to a 386SX computer, while the controllers are implemented in software developed in "C" language. A PC-LAB card (PC-LAB 718), which provides analog-to-digital and digital-to-analog conversion facilities, is used to communicate with the robot. This communication involves a multiplexing protocol using hardware that was developed in-house. Limit switches are used to disable the motors in case the robot reaches its limits.

A single link of the experiment was used to illustrate the proposed controllers. First, the system was controlled using a simple PD feedback controller which damps out vibration, and which can be proved to be asymptotically stable using the work–energy rate principle [6]. The feedback gains were chosen to produce an underdamped response. The reference input to the system is a step input corresponding to a 90 degree slew. The rigid body motion of the system containing large overshoot and small damping is illustrated in Figure 3(a). The time response of the tip of the link from the rigid body position is shown in Figure 3(b). Two frequencies are evident in the response: the low frequency is the contribution of the underdamped rigid body response and the high frequency is the first mode of vibration of the link. The control input to the system varies harmonically with small amplitude, high frequency content due to the coupling of the flexible modes and the rigid body mode superimposed on the gross low frequency (Figure 3(c)). The arc length

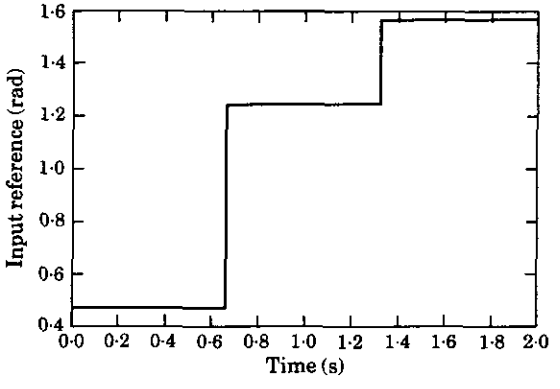

Figure 4. Reference input for the three-impulse/PD controller.

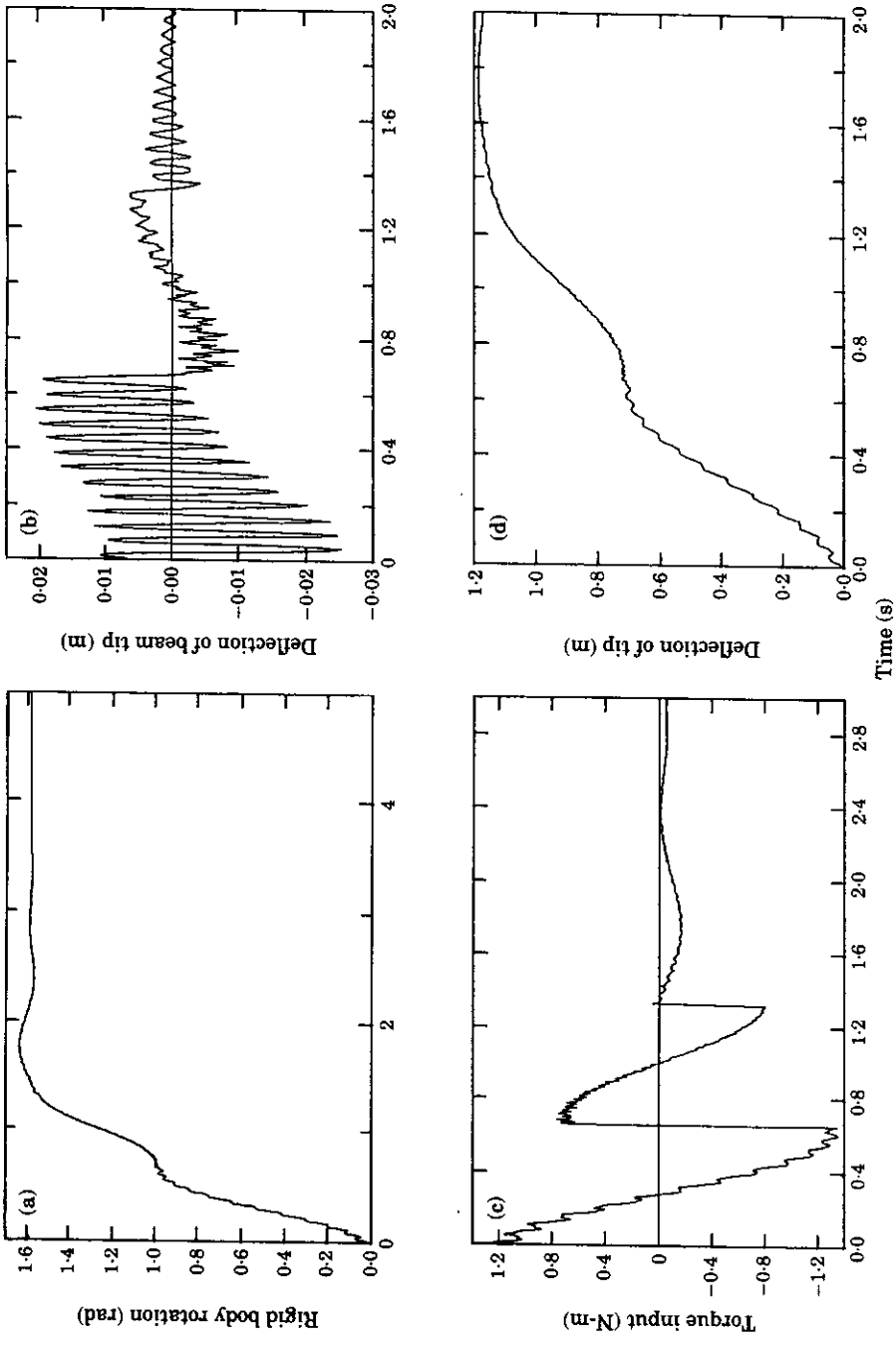

Figure 5. Experimental results of a three-impulse/PD controller: (a) rigid body response; (b) tip deflection of link; (c) control input history; (d) arc traversed by tip of link.

TABLE 3

Nine-impulse sequence convolved with a step input

Time (s)	Amplitude of step (rad)
0·0	0·1046
0·0242	0·3103
0·0484	0·3994
0·6549	0·6109
0·6791	1·0033
0·7033	1·1962
1·3098	1·2913
1·3339	1·4785
1·3581	1·5707

described by the tip of the link is shown in Figure 3(d). This is not very different from Figure 3(a), stating that the absolute value of the tip deflection is small compared to the deflection due to the slew.

The next experiment involved elimination of the frequency corresponding to the rigid body motion. The three-impulse-shaped input controller was designed to modify the reference input to the system. Convolution of the three-impulse with the reference input leads to the input sequence (Table 2) which is illustrated in Figure 4. The rigid body response (Figure 5(a)) reveals a very small overshoot and reaches the desired position in about two seconds. The manifestation of the first mode of vibration in the tip response is illustrated in Figure 5(b). A point to note is that the amplitude of the tip vibration has been significantly reduced compared to the previous controller. In Figure 5(c), the time history of the control input, it is shown that there are two switches in the sign of the control signal which correspond to the application of the multiple stepped input. The arc length of the tip of the link shows a response similar to the rigid body, but with a greater amplitude of the high frequency content (Figure 5(d)).

The next experiment involved elimination of the first two frequencies, leading to a nine-impulse sequence, shaped input controller. Convolving this impulse sequence with the reference input leads to the input sequence listed in Table 3.

The reference input to eliminate the two modes of vibration is shown in Figure 6. The rigid body response (Figure 7(a)) to this reference input is smoother than that shown in Figure 5(a). The tip deflection has a very small amplitude of vibration, and the deflection

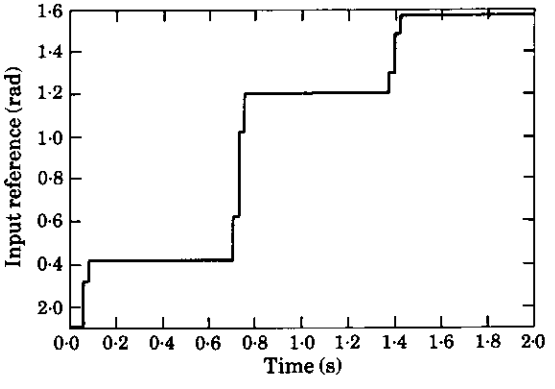

Figure 6. Reference input for the nine-impulse/PD controller.

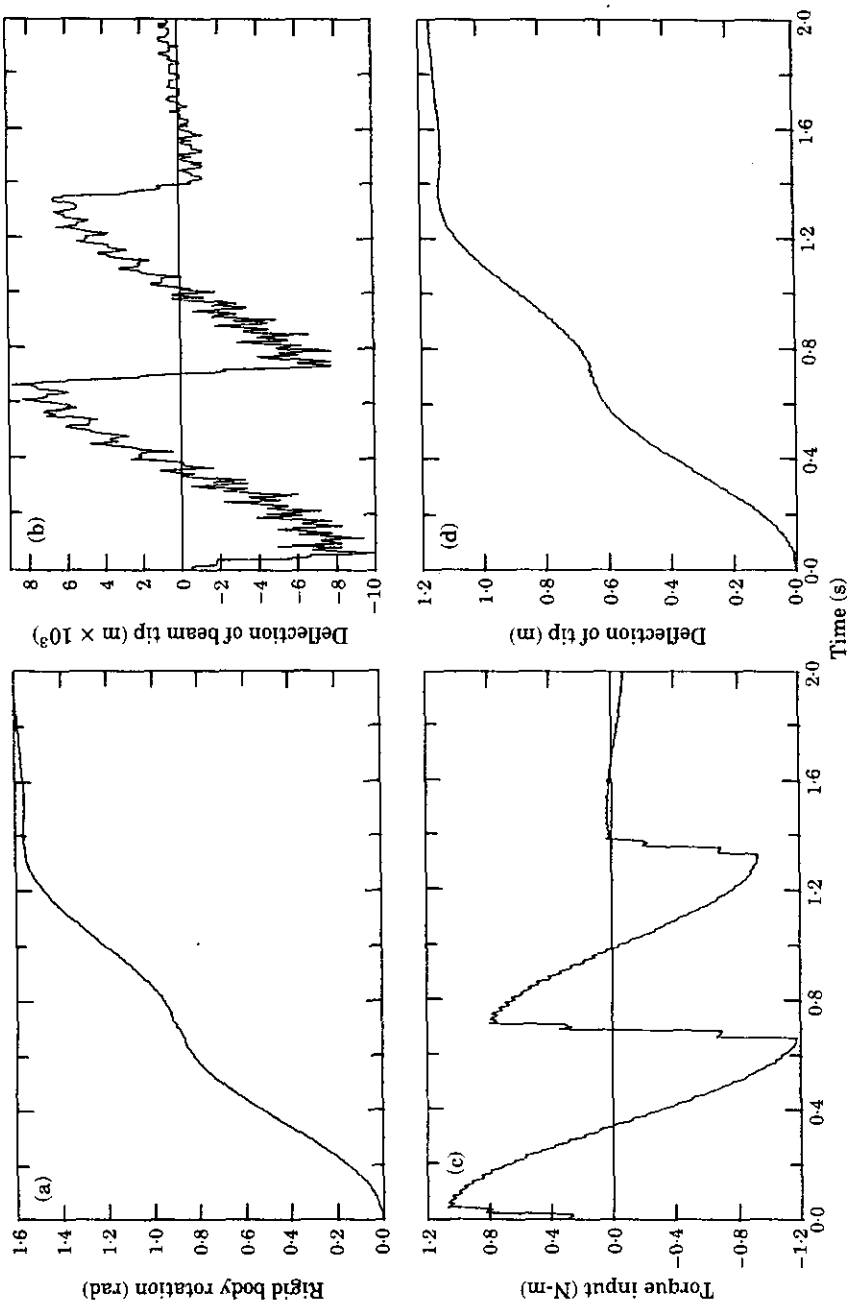

Figure 7. Experimental results of a nine-impulse/PD controller: (a) rigid body response; (b) tip deflection of link; (c) control input history; (d) arc traversed by tip of link.

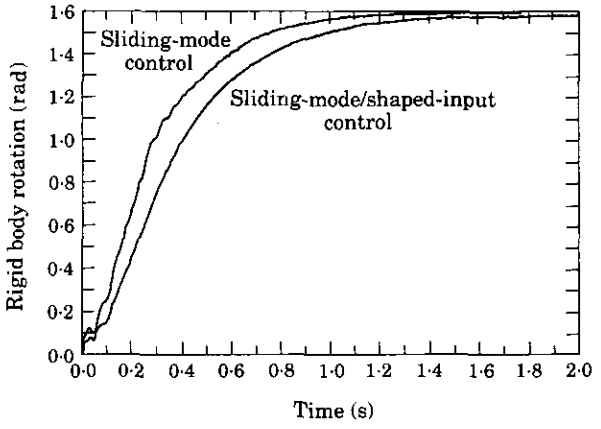

Figure 8. Experimental results of a sliding mode and sliding-mode/shaped-input controller: rigid body rotation.

of the tip is due to the minimum phase characteristic of the system (Figure 7(b)). The control input (Figure 7(c)) to the system contains sudden changes in magnitude at every instant of application of the impulse of the shaped-input controller.

The proposed shaped-input/sliding-mode control technique is next implemented on the single-link, flexible arm robot. In this technique, a sliding-mode controller is designed based on the rigid body model only. With this controller in place, the dynamics of the system are studied and any harmonics in the response are eliminated using input shaping. The rigid body model of the robot in question is

$$\dot{\mathbf{x}} = \begin{bmatrix} 0 & 1 \\ 0 & -0{\cdot}0599 \end{bmatrix} \mathbf{x} + \begin{bmatrix} 0 \\ 0{\cdot}0528 \end{bmatrix} u. \tag{20}$$

The surface

$$\sigma = [7{\cdot}2919 \quad 1]\mathbf{x} = 0 \tag{21}$$

produces a pole at $-7{\cdot}2919$ when the system state is sliding on the surface. The control law given by equation (13), with $\epsilon = 5{\cdot}7825$, provides us with poles at $s = -5{\cdot}78$ and $s = -7{\cdot}29$, which correspond to poles at $z = 0{\cdot}9715$ and $z = 0{\cdot}9642$ in the discrete domain. The feedback gains to achieve the poles in the continuous domain and the discrete domain are

$$K = [799{\cdot}0597 \quad 246{\cdot}6248], \qquad K = [773{\cdot}55 \quad 240{\cdot}67], \tag{22, 23}$$

respectively. The effect of this feedback gain on the continuous sixth order model of the system,

$$\dot{\mathbf{x}} = \begin{bmatrix} 0 & 0 & 0 & 1 & 0 & 0 \\ 0 & 0 & 0 & 0 & 1 & 0 \\ 0 & 0 & 0 & 0 & 0 & 1 \\ 0 & 139\,090 & 871\,680 & -3{\cdot}8716 & 0 & 0 \\ 0 & -58\,406 & -359\,970 & 1{\cdot}5988 & 0 & 0 \\ 0 & -9165{\cdot}7 & -9536{\cdot}3 & 0{\cdot}2551 & 0 & 0 \end{bmatrix} \mathbf{x} + \begin{bmatrix} 0 \\ 0 \\ 0 \\ 6988{\cdot}5 \\ -2886{\cdot}0 \\ 460{\cdot}5 \end{bmatrix} u, \tag{24}$$

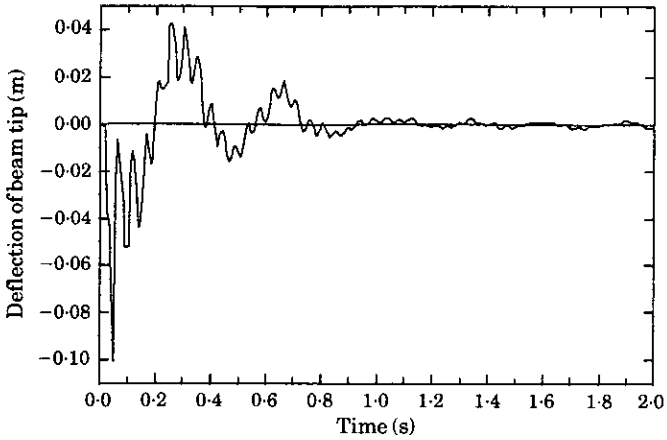

Figure 9. Experimental results of a sliding-mode controller: tip deflection.

is to produce poles at the locations $s = -0{\cdot}0165 \pm 31{\cdot}072\text{i}$, $-0{\cdot}0166 \pm 194{\cdot}74\text{i}$, $-3{\cdot}2145$ and $-1{\cdot}6819\text{E}6$. The poles at $-0{\cdot}0166 \pm 194{\cdot}74\text{i}$ are insignificant (with respect to frequency) compared to the poles at $-0{\cdot}0165 \pm 31{\cdot}072\text{i}$. The latter two poles produce a damped natural frequency of 31·072 rad/s. The input is shaped so that the vibration of frequency 31·072 rad/s is eliminated. The damping ratio of this mode is $5{\cdot}3\text{E} - 4$. Table 1 is used to determine the relative amplitudes and time of application of the three impulses to design the shaped input controller.

The response of the shaft of the motor (Figure 8) shows an exponential behavior. To better appreciate the controller performance, plots of the response of the system when only the sliding-mode controller is in place, and when both the sliding-mode and shaped-input (SM–SI) are in place, are overlaid, as shown in Figure 8. It can be seen from Figure 9 that the system with the rigid body controller sets up large amplitudes of vibration of the tip of the link, which show up in the arc traversed by the tip, as shown in Figure 10. The magnitude of the input torque required for the SM–SI controller is symmetric about the

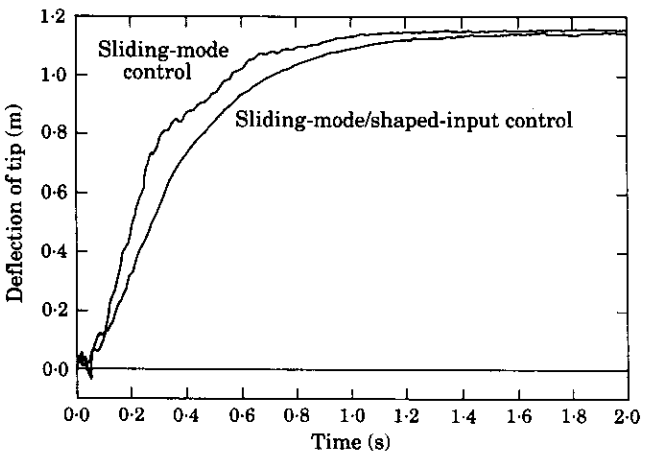

Figure 10. Experimental results of a sliding-mode and a sliding-mode/shaped-input controller: arc length traversed by the tip.

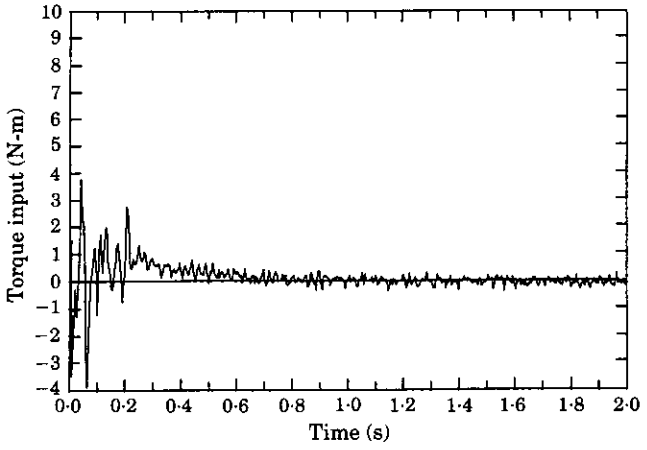

Figure 11. Experimental results of a sliding-mode/shaped-input controller: torque input.

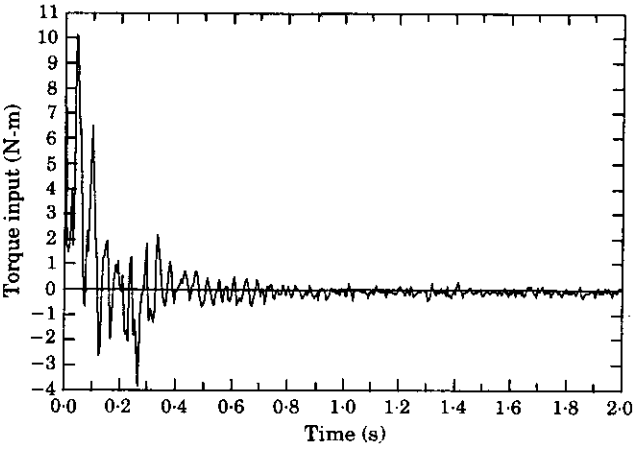

Figure 12. Experimental results of a sliding-mode controller: torque input.

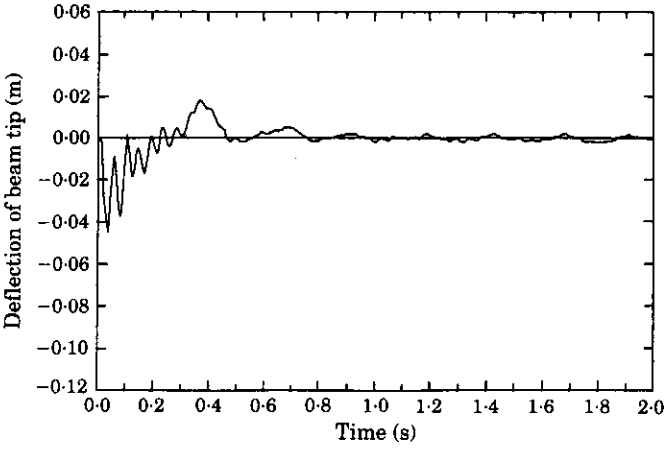

Figure 13. Experimental results of a sliding-mode/shaped-input controller: tip deflection.

origin (Figure 11), unlike the sliding-mode controller case (Figure 12). Thus, by dividing the input into multiple steps, the SM–SI technique provides us with more available torque to achieve a quicker response. Any discrepancy between the expected tip deflection and the actual response can be credited to the unmodelled dynamics of the velocity feedback circuit of the motor unit, which has been modelled as a simple gain. This could move the poles from the estimated position to a different location, leading to the oscillator behavior of the tip of the beam. The deflection of the beam tip for the SM–SI controller (Figure 13) is smaller than that for the sliding-mode controller by an order of magnitude, lending credibility to the filtering characteristic of the shaped-input controller.

5. CONCLUSIONS

A generalized scheme based on the sliding-mode and shaped-input concepts has been proposed for the control of flexible/rigid multi-link robots. The design process is two-fold; design of the rigid body motion controller followed by the design of a flexible motion attenuator.

The design of the controller for the rigid body motion requries selection of a hyperplane in state space which produces the desired dynamics. The controller is then designed such that the hyperplane selected is a globally attractive manifold and leads to a sliding mode. The selection of the control law to make the selected surface an attractive manifold is based on a Lyapunov function.

Once the rigid body controller is designed, the system equations, with the rigid body controller, are linearized about an operating point. The design of the shaped-input controller requires information about the natural frequency and damping of the linearized system. This information is used to modify the input such that the flexible modes are not excited.

The proposed control strategy has been implemented on an experimental single flexible link robot, where the damping of the structure was estimated experimentally using modal analysis. The results have proven the potential of this technique to control multi-flexible/rigid link robots.

REFERENCES

1. A. G. Butkovskii and A. Y. Lerner 1960 *Automation and Remote Control* **21**, 472–477. The optimal control of the systems with distributed parameters.
2. P. T. Kotnik, S. Yurkovich and Ü. Özguner 1984 *Journal of Robotic Systems* **5**, 181–196. Acceleration feedback for control of a flexible manipulator arm.
3. L. Meirovitch, H. Baruh, R. C. Montgomery and J. P. Williams 1984 *Journal of Guidance, Control and Dynamics* **7**, 437–442. Nonlinear natural control of an experimental beam.
4. C. M. Oakley and R. H. Cannon, Jr. 1989 *Proceedings of the* 1989 *American Control Conference* **2**, 1381–1388. End-point control of a two-link manipulator with a very flexible forearm: issues and experiments.
5. C. M. Oakley and R. H. Cannon, Jr. 1989 *Proceedings of the* 1989 *American Control Conference* **1**, 267–278. Equations of motion for an experimental planar two-link flexible manipulator.
6. S. R. Vadali, H. S. Oh and J. L. Junkins 1992 *Journal of Guidance Control and Dynamics* (in press). Use of the work–energy rate principle for designing feedback control laws.
7. G. Gebler, F. Pfeiffer and U. Kleemann 1988 *IFAC Proceedings Series, Robot Control*, 41–45. On dynamics and control of elastic robots.
8. N. C. Singer and W. P. Seering 1990 *American Society of Mechanical Engineers, Journal of Dynamics Systems, Measurement, and Control* **112**, 76–82. Preshaping command inputs to reduce system vibration.

9. T. SINGH, R. N. DUBEY and M. E. GOLNARAGHI 1990 *Proceedings of the CSME Mechanical Engineering Forum* 1990, *Toronto*. Sliding mode control of a single-link flexible arm robot.
10. W. E. SINGHOSE, N. C. SINGER and W. P. SEERING 1990 *Proceedings of the* 1990 *IEEE International Conference on Robotics and Automation* **2**, 922–927. Shaping input to reduce vibration: a vector diagram approach.
11. O. J. M. SMITH 1958 *Feedback Control Systems*. New York: McGraw-Hill.
12. V. I. UTKIN 1978 *Sliding Modes and Their Application in Variable Structure Systems*. Moscow: MIR.
13. M. VIDYASAGAR and D. WANG 1986 *Robotic Theory and Application*, 31–37. Modelling and control of flexible beam using the stable factorisation approach.
14. W. J. WILSON, R. A. DEACON and R. S. RAMSHAW 1986 *Proceedings of the Robotic Theory and Application, Winter Annual Meeting of American Society of Mechanical Engineers, Anaheim, California*, 31–37. Control of a single-link flexible arm experiment.